Evaluating the Error Probability in Lightwave Systems with Chromatic Dispersion, Arbitrary Pulse Shape and Pre- and Postdetection Filtering

Enrico Forestieri, *Member, IEEE*

***Abstract*—A novel approach to analytically evaluate the bit error probability in optically preamplified direct-detection systems is presented, which can take into account the effects of pulse shaping, chirping, filtering at the transmitter and the receiver, both pre- and postdetection, chromatic dispersion, and ASE noise. The method is computationally very fast in that the saddle point integration method for solving the resulting line integral of a particular moment generating function is adopted. A closed-form approximation for the bit error probability is also provided, which is within 0.01 dB from the exact numerical results.**

I. Introduction

THE PERFORMANCE evaluation in terms of bit error probability of a direct-detection lightwave communication system with an optical preamplifier has received much attention in the recent years (see [1]–[11] and references cited therein). Many of these works use approximations or simplified assumptions, such as the use of ideal NRZ formats [1]–[3], [5], [7], [11] and/or *ad hoc* combinations of pre- and postdetection filters, e.g., short-term integrator and discrete-time integrator [3], [7], or wide-band ideal filter and short-term integrator [1], [2], [4], [5], [9]. More general approaches are presented in [6], [8]–[10], but the method proposed in [6] is of difficult computability and neglects the intersymbol interference effects, in [8]–[9] the optical filter must be ideal with wide band, while the results in [10] hold only for a singly resonant type optical filter and the derived moment generating function is only used to find mean and variance of the decision sample whose statistics are arbitrarily assumed to be Gaussian. If the amplifier spontaneous noise dominates the receiver shot and thermal noises, the system performance will be identical to that of a radio system with square law detection and, to the author knowledge, the most comprehensive work in this case is that in [12] where, however, it is required that the input spectral densities are of rational form and the post-detection filter has a non negative impulse response. So, to our knowledge, there is no theory available which accurately takes into account arbitrary signal pulse shape, chirping, filtering at the transmitter and the receiver, both pre- and postdetection, and chromatic dispersion. We present here a novel approach to analytically evaluate the bit error probability in preamplified direct detection systems, which aims at filling some of the remaining gaps and giving accurate results. This approach employs the moment generating function of the output and the saddle point integration method and in this respect is similar to that in [12], but overcomes its computational difficulties (a set of differential equations of the Kalman–Bucy type is to be numerically solved) and limitations by considering a periodic input signal instead that the completely arbitrary one there considered.

This paper is organized as follows. In Section II the model used in the analysis is presented. In Section III it is shown how signal and noise may be expanded to take into account arbitrary filtering. The bit error probability is evaluated in Section IV through the saddle point integration method and a closed-form saddle point approximation is provided. Numerical results are presented in Section V to show the effectiveness of the proposed method.

II. System Model

The system model is shown in Fig. 1. The optical signal generated by a laser modulator is launched in a singlemode fiber operated in linear regime. At the receiver end it is amplified by a flat gain G erbium-doped fiber amplifier which adds amplified spontaneous emission (ASE) noise and then the amplifier output is optically filtered prior photodetection. The photodetection process and the following electronic circuitry will add shot and thermal noise, respectively. The detected signal is then low—pass filtered and sampled.

The ASE noise is modeled as additive white Gaussian noise (AWGN) with one sided power spectral density $N_{ss} = n_{sp}(G-1)h\nu$ in each polarization [1] where $n_{sp} \geq 1$ is the spontaneous emission parameter and $h\nu$ is the photon energy. By using high-gain amplifiers the ASE noise dominates the shot and thermal noises generated in the receiver [1] and thus they can be neglected. Then, in the absence of fiber nonlinearities and polarization dispersion, assuming there is no ASE in the orthogonal polarization, the direct detection lightwave system has the low-pass equivalent model shown in Fig. 2. Here $x(t)$ is the low-pass equivalent (also referred to as complex envelope) of the transmitted signal as defined in [13], $w(t)$ is a complex AWGN with twosided power spectral density

$$N_0 = n_{sp}\frac{G-1}{G}h\nu \simeq n_{sp}h\nu \qquad \text{for } G \gg 1. \tag{1}$$

Manuscript received September 27, 1999; revised August 4, 2000. This work was supported by Marconi Communications under Contract 353/23304.

The author is with the Dipartimento di Ingegneria dell'Informazione, Università di Parma, I-43100 Parma, Italy.

Publisher Item Identifier S 0733-8724(00)09815-7.

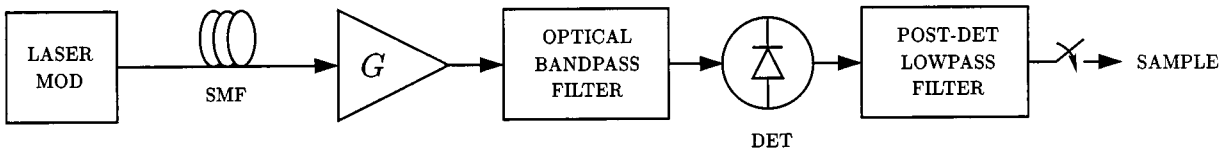

Fig. 1. System model.

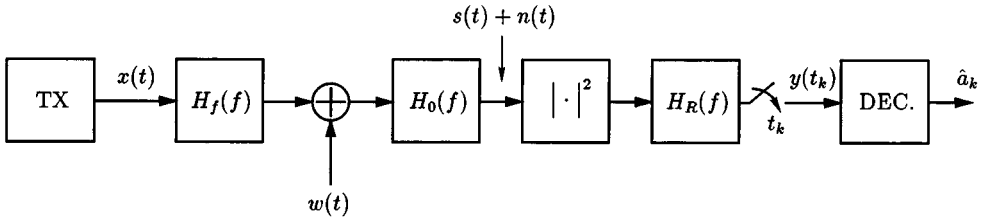

Fig. 2. Equivalent low-pass system model.

$H_f(f), H_0(f)$ and $H_R(f)$ are the (low-pass equivalent) transfer functions of fiber and optical and postdetection filters, respectively.

In the absence of nonlinearities and polarization dispersion, the equivalent low-pass transfer function of a lossless linear dispersive singlemode fiber of length L can be written as $H(f) = e^{-j\beta'(f)L}$ where $\beta'(f) \triangleq \beta(f+\nu)$ and $\beta(f)$ is the propagation constant. Taking the Taylor series expansion of $\beta(f)$, neglecting the constant and linear terms in f (as they do not introduce distortion) and the dispersion terms of order greater than two, the fiber can be modeled as a bandpass filter whose transfer function has flat amplitude response and quadratic group delay inside the signal bandwidth and is zero outside. This assumption is valid when the signal bandwidth is narrow with respect to the value of the optical carrier frequency.

Then, inside the signal bandwidth, with very good approximation the equivalent low-pass transfer function of the dispersive fiber can be taken to be

$$H_f(f) = e^{-j[(1/2)\beta_2'\omega^2 + (1/6)\beta_3'\omega^3]L} \tag{2}$$

where $\omega = 2\pi f$ for shortness and

$$\beta_2' \triangleq -\frac{\lambda^2}{2\pi c} D \tag{3}$$

$$\beta_3' \triangleq \left(\frac{\lambda}{2\pi c}\right)^2 (2\lambda D + D'\lambda^2). \tag{4}$$

In the expressions above c is the light speed, λ is the optical wavelength corresponding to the carrier frequency, D is the fiber chromatic dispersion parameter at λ [usually provided in ps/(km·nm)] and $D' = dD/d\lambda$ evaluated at λ, too. However, notice that the parameter β_3' is non negligible only if $|\beta_2'/\beta_3'| \lesssim R_b$ [14] where R_b is the bit rate, i.e. if $D' \gtrsim 2((\pi c/\lambda R_b) - 1)(D/\lambda)$. For $R_b = 10$ Gb/s, $\lambda = 1550$ nm, expressing D in ps/(km·nm) and D' in ps/(km·nm^2) this imply $D' \gtrsim 7.8 \cdot 10^4 D$. For a nondispersion shifted fiber typically $D \approx 17$ ps/(km·nm) and $D' \approx 0.083$ ps/(km·nm^2) and thus β_3' is negligible and the fiber group delay can be considered to be linear.

III. Signal and Noise Expansions

As regards of the signal $x(t)$, given a N-bit sequence $\{a_n\}$ to be transmitted and the elementary pulse $p(t)$, we take it to be the periodic repetition, with period NT, of the actual PAM signal

$$d(t) = \sum_{i=0}^{N-1} a_i p(t - iT) \tag{5}$$

i.e.,

$$x(t) = \sum_{n=-\infty}^{\infty} d(t - nNT). \tag{6}$$

When N is sufficiently large, $x(t)$ in (6) is a pseudorandom signal which allows for mathematical tractability while retaining physical properties close to reality. Moreover, an appropriate choice of the sequence $\{a_n\}$, such as a de Bruijn sequence [15], allows us to take easily into account the effects of intersymbol interference. Due to its periodicity, $x(t)$ may be expanded in Fourier series

$$x(t) = \sum_{\ell=-\infty}^{\infty} x_\ell e^{j2\pi\ell t/NT} \tag{7}$$

where

$$x_\ell = \frac{1}{NT} P\left(\frac{\ell}{NT}\right) \sum_{m=0}^{N-1} a_m e^{-j2\pi\ell m/N} \tag{8}$$

and $P(f)$ is the Fourier transform of $p(t)$.

As regards of noise, observe that when the overall impulse response of the pre- and postdetection filters at the receiver has a finite time duration, say equal to T_0, then the value of the sample $y(t_k)$ is solely determined by the values that the input waveform of the optical filter takes on in the time interval $(t_k - T_0, t_k)$. Theoretical filters may not have finite duration impulse responses, but from a practical point of view all *real* filters do have finite impulse responses. So, if we take their practical overall impulse response duration equal to T_0 we could replace their input waveform with another one which coincides only in the time interval $(t_k - T_0, t_k)$, leaving the value of the sample $y(t_k)$ unchanged, as said. This means that an exact description of the input noise waveform in the aforementioned time interval

is a sufficient statistics. So we may write a Karhunen–Loève expansion for $w(t)$ in the interval $t_k - T_0 < t < t_k$ only, and, as $w(t)$ is AWGN, we can choose any orthonormal base for the expansion [16], [17], for example the Fourier base $\{\varphi_m(t) = (1/\sqrt{T_0})e^{j2\pi m(t-t_k+T_0)/T_0}\}_{m=-\infty}^{\infty}$. So the relevant noise process becomes $w(t) = \sum_{m=-\infty}^{\infty}\omega_m\varphi_m(t)$, $t_k - T_0 < t < t_k$, where ω_m are complex independent and identically distributed (i.i.d.) Gaussian random variables (r.v.) with zero mean and in-phase and quadrature components of variance $N_0/2$. For convenience we rewrite $w(t)$ as

$$w(t) = \sum_{m=-\infty}^{\infty} w_m e^{j2\pi m(t-t_k+T_0)/T_0} \quad t_k - T_0 < t < t_k \tag{9}$$

where w_m are complex i.i.d. Gaussian r.v. with zero mean and in-phase and quadrature components of variance

$$\sigma^2 = \frac{N_0}{2T_0}. \tag{10}$$

The value of T_0 depends upon the optical and postdetection filters and we will see how it can be easily determined.

We now have all the ingredients to evaluate the sample $y(t_k)$ and thus the bit error probability.

IV. Bit Error Probability

After some laborious calculations, detailed in Appendix A, we show that the sample $y(t_k)$ at the input of the decision device may be written as

$$y(t_k) = d_k + r_k \tag{11}$$

where

$$d_k \triangleq \sum_{\ell=-2L}^{2L} c_\ell H_R\left(\frac{\ell}{NT}\right) e^{j2\pi\ell t_k/NT} \tag{12}$$

is the signal term, $L = \eta N B_{0N} T$, B_{0N} being the noise equivalent bandwidth of $H_0(f)$ (i.e., half the noise equivalent bandwidth of the optical filter), η a small number (whose value is chosen such that to retain all the relevant harmonics), and c_ℓ is given in (A.8), while r_k is the noise term which may be written as

$$r_k = n_k - \nu_k \tag{13}$$

where

$$n_k \triangleq \sum_{i=1}^{2M+1} \lambda_i \left| z_i + \frac{b_i}{\lambda_i}\right|^2 \tag{14}$$

$$\nu_k \triangleq \sum_{i=1}^{2M+1} \frac{|b_i|^2}{\lambda_i} \tag{15}$$

with $M = \eta B_{0N} T_0$, λ_i are the eigenvalues of the $(2M+1)\times(2M+1)$ Hermitian matrix A in (A.20), the complex random variables $z_i = z_{Pi} + jz_{Qi}$ are zero mean Gaussian with independent in-phase and quadrature components of variance σ^2 as in (10), b_i are the components of the complex vector $\mathbf{b}$ given in (A.26).

Despite the seeming complexity, all the quantities involved in the evaluation of the sample $y(t_k)$ in (11) are easily obtainable numerically.

The noise sample n_k is a noncentral quadratic form of Gaussian random variables, for which it can be easily shown that its moment generating function (MGF) is[1]

$$\Psi_{n_k}(s) = \prod_{i=1}^{2M+1} \frac{\exp\left(\dfrac{\alpha_i s}{1-\beta_i s}\right)}{1-\beta_i s} \tag{16}$$

where

$$\alpha_i \triangleq \frac{|b_i|^2}{\lambda_i} \tag{17}$$

$$\beta_i \triangleq 2\lambda_i\sigma^2 \tag{18}$$

and its mean and variance are

$$\eta_{n_k} = \sum_{i=1}^{2M+1}(\alpha_i+\beta_i) = \sum_{i=1}^{2M+1}\left(2\lambda_i\sigma^2 + \frac{|b_i|^2}{\lambda_i}\right) \tag{19}$$

$$\sigma_{n_k}^2 = \sum_{i=1}^{2M+1}\beta_i(2\alpha_i+\beta_i) = \sum_{i=1}^{2M+1} 4\sigma^2(\lambda_i^2\sigma^2 + |b_i|^2). \tag{20}$$

Setting the decision threshold to $\gamma_t h$, the probability of error at the sampling time t_k, conditional upon the information sequence $\{a_n\}$, is

$$P(e_k|\{a_n\}) = \begin{cases} P\{y(t_k) < \gamma_{th}\} = P\{n_k < \xi_k\}, & a_k = 1 \\ P\{y(t_k) > \gamma_{th}\} = P\{n_k > \xi_k\}, & a_k = 0 \end{cases} \tag{21}$$

where

$$\xi_k = \gamma_{th} - d_k + \nu_k \tag{22}$$

and the average probability of error P_b can be expressed as

$$P_b = \frac{1}{N}\sum_{k=0}^{N-1} P(e_k|\{a_n\}). \tag{23}$$

The average transmitted (and received, for a lossless fiber) energy per bit is

$$\begin{aligned} E_b &= T\int_{-\infty}^{\infty} S_x(f)\,df \\ &= \frac{1}{2}\int_{-\infty}^{\infty}|P(f)|^2 df + \frac{1}{4T}\sum_{k=-\infty}^{\infty}\left|P\left(\frac{k}{T}\right)\right|^2 \end{aligned} \tag{24}$$

where $S_x(f)$ is the signal power spectrum, and the signal to noise ratio E_b/N_0 represents the number of signal photons per bit at the input of the ideal high-gain optical amplifier.

We show in Appendix B that the probabilities that appear in (21) may be evaluated as

$$P\{n_k > \xi_k\} = \frac{1}{2\pi j}\int_{u_0-j\infty}^{u_0+j\infty}\frac{\Psi_{n_k}(s)}{s}e^{-s\xi_k}\,ds \qquad 0 < u_0 < \frac{1}{\max\beta_i^+} \tag{25}$$

[1]If there is ASE in the orthogonal polarization, to the noise sample n_k in (14) should be added the additional term $\sum_{i=1}^{2M+1}\lambda_i|z_i'|^2$ where the z_i''s are independent r.v. distributed as the z_is. So in this case the MGF would be as in (16) but replacing the term $(1-\beta_i s)$ with $(1-\beta_i s)^2$ in the denominator of the main fraction only.

$$P\{n_k < \xi_k\} = -\frac{1}{2\pi j}\int_{u_0-j\infty}^{u_0+j\infty} \frac{\Psi_{n_k}(s)}{s} e^{-s\xi_k}\, ds \qquad -\frac{1}{\max|\beta_i^-|} < u_0 < 0 \tag{26}$$

where β_i^+ and β_i^- stands for the positive and negative β_is in (18), respectively. If all β_is are positive then the range in (26) is to be interpreted as $-\infty < u_0 < 0$. Notice that as the MGF is analytic in its regularity domain, from a theoretical point of view a particular choice of u_0 in the above ranges does not matter, but if the line integrals in (25) and (26) are to be evaluated numerically, it can make a world of difference. As the line integral of an analytic complex function does not depend on the path, if we could choose the path in such a way that along it the function real part achieves a sharp maximum while the imaginary part remains constant (to avoid rapid oscillations in the integrand) then the major contribution to the integral would come from the path section in the neighborhoods of the function real part maximum. The real and imaginary part of an analytic complex function cannot have maxima or minima but they can have saddle points which can be exploited in the numerical evaluation of (25) and (26). In Appendix B we show the details of this well known [18], [19] method of numerical integration through a saddle point along the path of steepest descent applied to the present case.

It can be shown that the integrand in (25) and (26) has two saddle points $u_0^- < 0$ and $u_0^+ > 0$ on the real s-axis which, once determined, can be used to obtain the closed-form *saddlepoint approximation* for the bit error probability. By writing (16) as $\Psi_{n_k}(s) = \exp[\Phi_{n_k}(s)]$ and expanding $\Phi_{n_k}(s)$ in power series about $u_0^\pm$ retaining terms up to s^2, (25) and (26) can be reduced to Gaussian integrals, which are evaluated to give the saddlepoint approximation [19]

$$P\left\{n_k \gtrless \xi_k\right\} \simeq \pm \frac{\exp\left[\Phi_{n_k}\left(u_0^\pm\right)\right]}{\sqrt{2\pi\Phi''_{n_k}\left(u_0^\pm\right)}} = \frac{\left[\Psi_{n_k}\left(u_0^\pm\right)\right]^{3/2} e^{-u_0^\pm \xi_k}}{\sqrt{2\pi\left[\left(u_0^\pm\right)^2 \Psi''_{n_k}\left(u_0^\pm\right) + \Psi_{n_k}\left(u_0^\pm\right)\right]}} \tag{27}$$

where Ψ''_{n_k} stands for the second derivative of Ψ_{n_k} and u_0^+ or u_0^- must be used for the $>$ or $<$ sign, respectively. We found that the saddle point approximation, which is the first term of an asymptotic expansion of (25) and (26), is very accurate and overestimates the true error probability for a factor corresponding to less than 0.01 dB on E_b/N_0 at error probabilities lower than 10^{-6}.

V. Results

In order to better appreciate the potential of the proposed method, we show in the following some numerical results for some typical cases.

Our method requires the determination of T_0 in (9), as previously pointed out. As a filter impulse response time duration is related to its bandwidth, we take T_0 as

$$T_0 = \mu\left(\frac{1}{B_{0N}} + \frac{1}{B_{RN}}\right) \tag{28}$$

where B_{0N} and B_{RN} are the noise equivalent bandwidths of the optical lowpass equivalent $H_0(f)$ and postdetection $H_R(f)$ filters, respectively, and μ is a dimensionless parameter which must be determined. In practice we repeatedly evaluate the bit error probability for increasing values of μ until the result stabilizes. This procedure may seem rough and time consuming, but it turns out to be instead very simple and effective.

All the results shown here were obtained by specifying the sequence $\{a_n\}$ as a 2^5-bit de Bruijn sequence [15]. In this sequence all 5–bit patterns occur exactly once in a single period and thus it is possible to accurately account for intersymbol interference due to two bits on either side of the desired bit (or the preceding four bits) and this is more than adequate in our case.

As a first example, let us consider a standard NRZ PAM signal, a nondispersive fiber, a matched optical filter and no post-detection filter (or, equivalently, a post-detection filter with a very large bandwidth). In this case it is known [20] that the exact error probability is given by

$$P_b = \tfrac{1}{2}\left[e^{-\xi/N_0} + 1 - Q\left(2\sqrt{E_b/N_0},\ \sqrt{2\xi/N_0}\right)\right] \tag{29}$$

where $Q(a, b) \triangleq \int_b^\infty x e^{-(a^2+x^2)/2} I_0(ax)\, dx$ is the Marcum Q-function [19], $I_0(x)$ being the modified Bessel function of the first kind and order zero, and ξ is the optimum threshold given implicitly by

$$I_0\left(2\sqrt{2\xi E_b}/N_0\right) = e^{2E_b/N_0}. \tag{30}$$

For very high values of E_b/N_0, using for $I_0(x)$ the crude approximation $I_0(x) \approx e^x$, we get $\xi \approx E_b/2$ and $P_b \approx (1/2)e^{-E_b/(2N_0)}$. This last expression, however, is only asymptotically exact and for small to medium values of E_b/N_0, overestimates the bit error probability for a factor of about two, so we will use (29) with the value of ξ obtained by numerically solving (30). Letting $\gamma = (E_b/N_0)_{\rm dB}$, we found that the optimum threshold is very well fitted by

$$\xi \approx \tfrac{1}{2}E_b \exp[1.156\exp(-0.145\gamma - 0.0015\gamma^2)] \quad \text{for } 2 < \gamma < 20. \tag{31}$$

In Figs. 3 and 4 the exact error probability is shown together with the results obtained by applying the present analysis to this case with μ and η, respectively, as parameters and with the threshold optimized for each E_b/N_0. The exact value of the error probability is obtained for $\mu = 1$ and values $\mu > 1$ all give the same curve which is practically coincident with the exact one. Notice that the asymptotic true value of the error probability is reached for $\mu = 1$ corresponding to $T_0 = T$, the exact duration of the matched filter impulse response.

As a second example, the results obtained for non dispersive fiber with Gaussian optical end postdetection filters are shown in Figs. 5 and 6 with μ and η as parameters. The optical and postdetection filter 3 dB bandwidths are such that $B_0T = 8$ and $B_RT = 0.7$, respectively [B_0 is twice the 3 dB bandwidth of $H_0(f)$]. In this and all other figures the performance curves shown are obtained with the threshold optimized for each E_b/N_0. The curves with μ as a parameter were obtained first by choosing for η a suitable value as explained in Appendix A, then μ was fixed and η varied for checking. As can be seen, for fixed η, the performance curves tend monotonically to a limiting

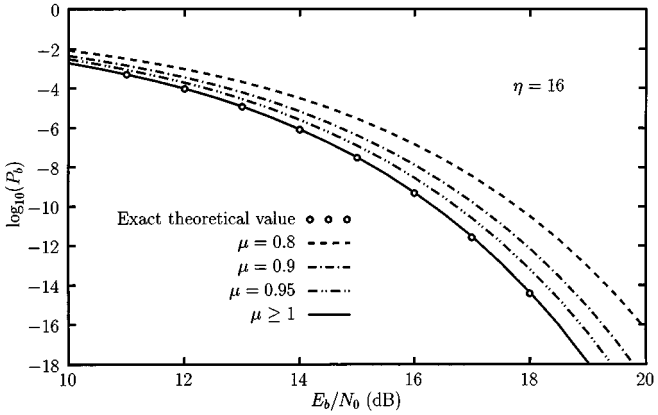

Fig. 3. Performance curves for increasing value of parameter μ. Nondispersive fiber and matched optical filter.

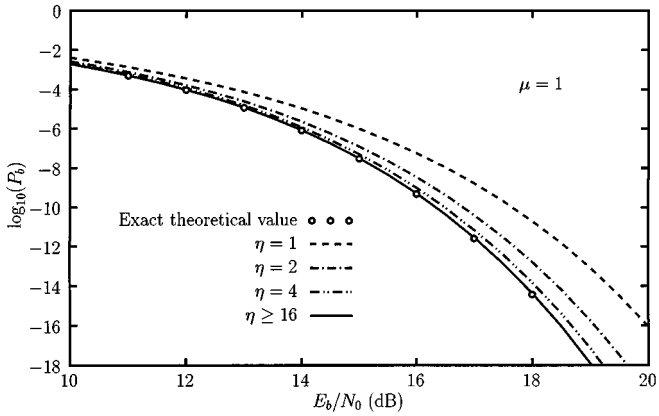

Fig. 4. Performance curves for increasing value of parameter η. Nondispersive fiber and matched optical filter.

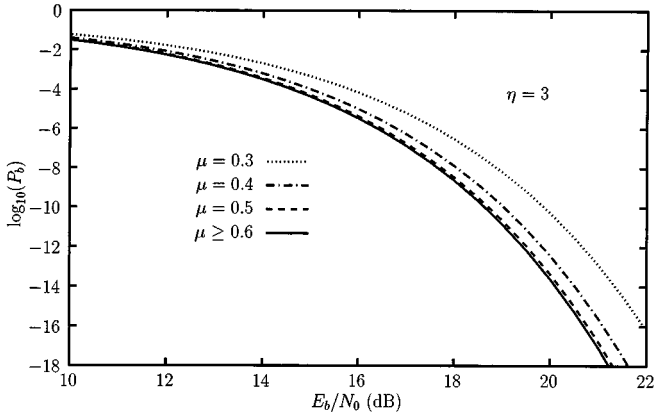

Fig. 5. Performance curves for increasing value of parameter μ. Nondispersive fiber, Gaussian optical and postdetection filters with 3-dB bandwidths such that $B_0T = 8$ and $B_RT = 0.7$, respectively.

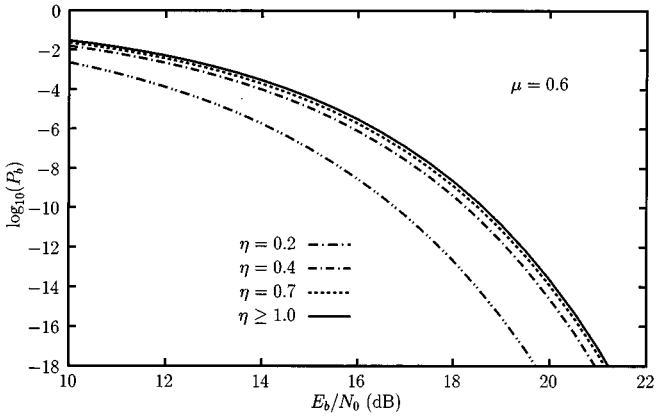

Fig. 6. Performance curves for increasing value of parameter η. Nondispersive fiber, Gaussian optical and postdetection filters with 3-dB bandwidths such that $B_0T = 8$ and $B_RT = 0.7$, respectively.

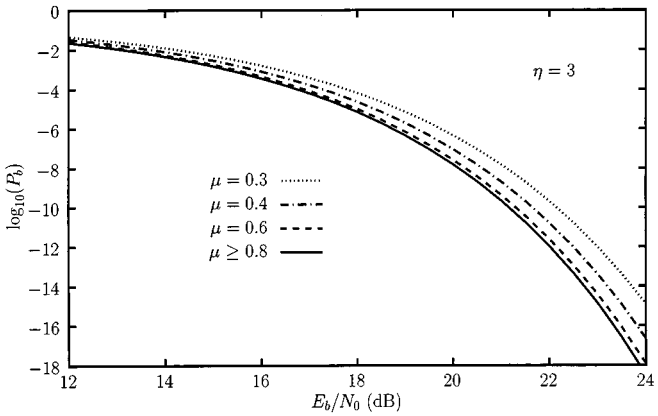

Fig. 7. Performance curves for increasing value of parameter μ. Nondispersive fiber, Gaussian optical filter with $B_0T = 8$ and RC-type postdetection filter with $B_RT = 0.7$.

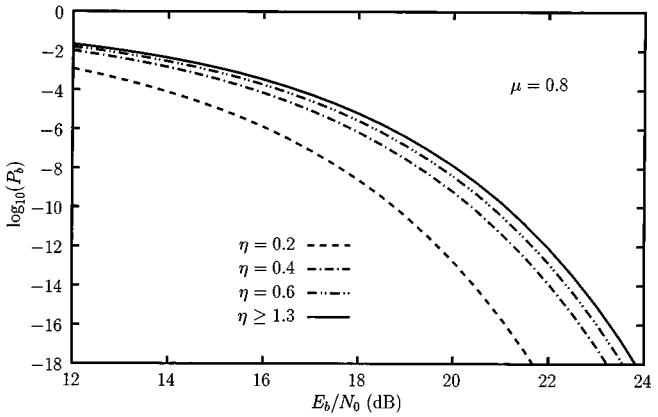

Fig. 8. Performance curves for increasing value of parameter η. Nondispersive fiber, Gaussian optical filter with $B_0T = 8$ and RC-type postdetection filter with $B_RT = 0.7$.

curve which is already reached for $\mu = 0.6$. We observed that this is a common behavior of all kinds of postdetection filters with impulse responses which do not change sign, i.e., filters for which the matrix A in (A.20) is positive definite. This, for example, is also the case for a RC-type (one pole) post-detection filter, to which Figs. 7 and 8 refers. In this case the limiting curve is already reached for $\mu = 0.8$.

Postdetection filters whose impulse response change sign exhibit another kind of behavior as, for increasing values of μ, the curves go initially in a direction, then after an inversion of direction they tend monotonically to the limiting curve. This is explained by the fact that considering an increasing duration of the impulse response we arrive at a point when the negative portion of the impulse response comes into play. Figs. 9 and 10 show the

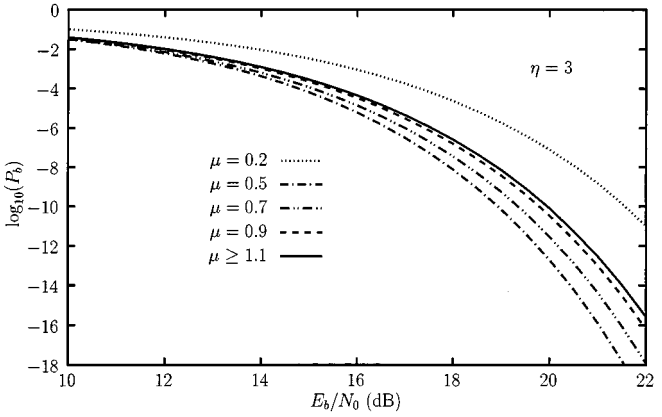

Fig. 9. Performance curves for increasing value of parameter μ. Nondispersive fiber, Gaussian optical filter with $B_0T = 8$ and second-order Butterworth postdetection filter with $B_RT = 0.7$.

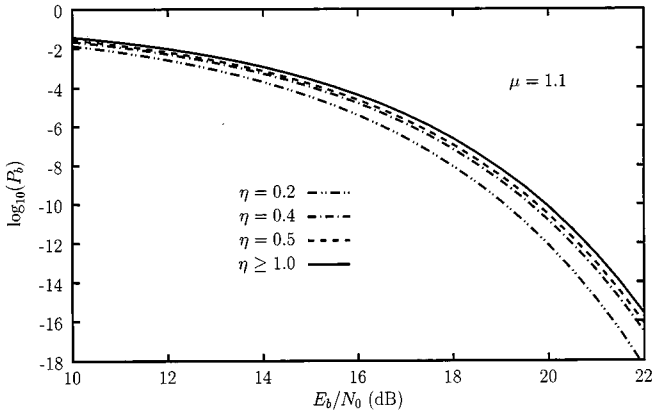

Fig. 10. Performance curves for increasing value of parameter η. Nondispersive fiber, Gaussian optical filter with $B_0T = 8$ and second-order Butterworth postdetection filter with $B_RT = 0.7$.

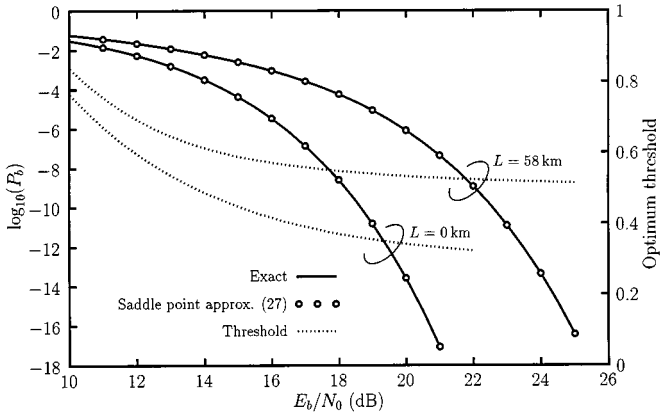

Fig. 11. Performance curves for a dispersive fiber. $R_b = 10$ Gb/s, $D = 17$ ps/nm·km, $\lambda = 1550$ nm, Gaussian optical and postdetection filters with $B_0T = 8$ and $B_RT = 0.7$, respectively. Curves are obtained with $\mu = 0.6$ and $\eta = 2$.

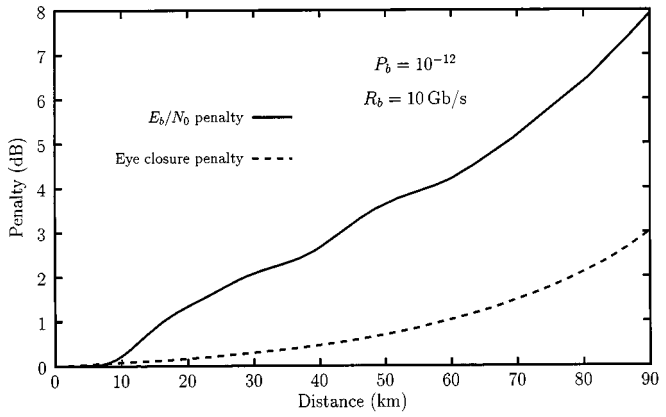

Fig. 12. E_b/N_0 penalty at $P_b = 10^{-12}$. Parameters are as in Fig. 11.

results obtained with a second-order Butterworth filter for which the limiting curve is reached for $\mu = 1.1$ and is not the leftmost curve in Fig. 9 but the second from right (the solid one). Similar results were observed with a sixth order Butterworth filter for which the limiting curve was reached for $\mu = 1.8$. As a general rule of thumb we observed that, when the bandwidth of the optical filter is large and the postdetection filter has not a too sharp cutoff, a value of $\mu = 2$ is more than adequate, otherwise a value of $\mu = 4$ is sufficient in almost all practical cases.

The results in Fig. 11 are relative to a dispersive fiber with $D = 17$ ps/nm·km, $\lambda = 1550$ nm, $R_b = 10$ Gb/s, Gaussian optical and postdetection filters with 3-dB bandwidths $B_0T = 8$ and $B_RT = 0.7$, and show the probability of error for a back-to-back configuration and after $L = 58$ km. The circles represent the probability of error evaluated by the saddle point approximation (27) while the dotted curves (whose values should be read on the right) represent the optimum threshold. As anticipated, the saddle point approximation is practically coincident with the true error probability and gives the correct value for the optimum threshold, too. As can be seen from the same figure, the fiber chromatic dispersion dictates the use of a higher threshold.

The usefulness of a fast accurate method for evaluating the error probability in the general case is underlined by the penalty curves, which can be drawn easily at any given P_b. For the same set of parameters of Fig. 11, we show in Fig. 12 the E_b/N_0 penalty at $P_b = 10^{-12}$ for a 10-Gb/s system. The popular eye closure penalty [21]–[25] curve is superimposed for comparison. The eye closure penalty is defined as $\Delta P_{eye} = 10\log_{10}(a/b)$, where a is the eye opening at the post-detection filter output with no fiber ($L = 0$ km) in place, and b is the eye opening with the fiber in place. It is evident that the eye closure penalty criterion fails completely in predicting the true penalty, as for example for $L = 40$ km it predicts 0.5-dB penalty while the true penalty is about 2.5 dB. The reason for this failure may be explained in the following way. The motivation behind the eye closure penalty criterion is that given the eye opening $V_1 - V_0$, where V_1 is the lowest level corresponding to a "1" and V_0 the highest level corresponding to a "0," assuming the noise is Gaussian with standard deviations σ_1 and σ_0 when transmitting a "1" or a "0," respectively, and setting the threshold so that the probability of error is equal for both "1" and "0" [26], we have that $P_b \leq (1/2)\mathrm{erfc}((V_1 - V_0)/(\sqrt{2}(\sigma_1 + \sigma_0)))$. So it may seem that effectively the eye opening can give the exact penalty. But, even approximating the noise as Gaussian, one should consider that σ_1, and σ_0 also depend on the value of V_1 and V_0, and then if V_1 gets decremented by $\Delta V_1 > 0$ and

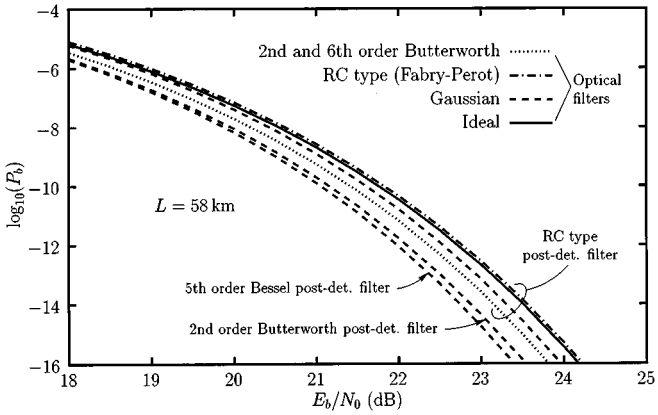

Fig. 13. Performance curves for a dispersive fiber and several optical and postdetection filter types. $R_b = 10$ Gb/s, $D = 17$ ps/nm·km, $\lambda = 1550$ nm, optical and post-detection filters with 3-dB bandwidths such that $B_0T = 1$ and $B_RT = 0.5$, respectively. Curves are obtained with the following parameters (optical filter/postdetection filter): $\mu = 0.8$ and $\eta = 3$ for Gaussian/Bessel, Gaussian/second-order Butterworth and Gaussian/RC; $\mu = 0.9$ and $\eta = 4$ for second-order Butterworth/RC; $\mu = 1.9$ and $\eta = 2$ for sixth-order Butterworth/RC; $\mu = 24$ and $\eta = 1$ for Ideal/RC; $\mu = 1$ and $\eta = 4$ for RC/RC.

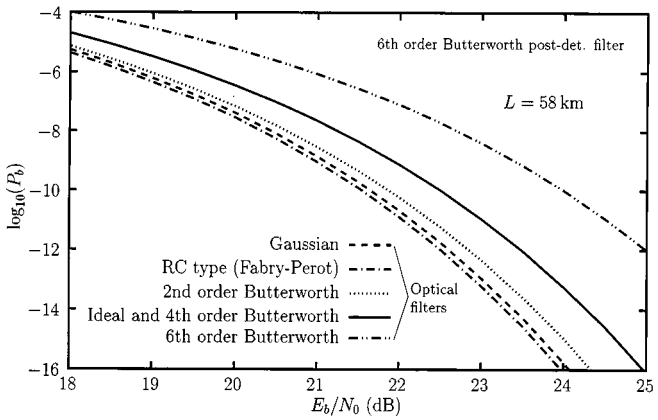

Fig. 14. Performance curves for a dispersive fiber, several optical filter types and sixth-order Butterworth postdetection filter. $R_b = 10$ Gb/s, $D = 17$ ps/nm·km, $\lambda = 1550$ nm, optical and postdetection filters with 3-dB bandwidths such that $B_0T = 1$ and $B_RT = 0.5$, respectively. Curves are obtained with the following parameters (only optical filter is specified): $\mu = 1.6$ and $\eta = 3$ for Gaussian; $\mu = 1.9$ and $\eta = 4$ for RC; $\mu = 2$ and $\eta = 3$ for second-order Butterworth; $\mu = 10$ and $\eta = 1$ for Ideal; $\mu = 2$ and $\eta = 2$ for fourth- and sixth-order Butterworth.

V_0 incremented by $\Delta V_0 > \Delta V_1$ this results in a penalty larger than that expected by the eye closure criterion. Moreover, the Gaussian approximation is very questionable when the signal level is low as in this case the noise $\times$ noise term may not be negligible with respect to the signal $\times$ noise one.

As a concluding example, the effect of different filter types is shown in Figs. 13 and 14 which refer to a dispersive fiber of length $L = 58$ km and where several different optical filters with the same narrow 3-dB bandwidth (such that $B_0T = 1$) were used together with several post-detection filters with $B_RT = 0.5$. These figures are representative of the dependence of the performance on the shape of the pre- and postdetection filters when both bandwidths are small with respect to the bit rate. It turns out that if using a postdetection filter with a smooth cutoff, the choice of the optical filter is not very important as the performance is always within 0.4 dB (given the same postdetection filter, since different couples can give differences of about 1 dB). But more care should be taken in selecting the optical filter when the postdetection one has a sharp cutoff, since a bad choice can result in a penalty of more than 2 dB, as can be seen from Fig. 14 in which the postdetection filter is a sixth-order Butterworth one. In this latter case it is important that the optical filter has a smooth cutoff or a phase as linear as possible, as evidenced by the fact that a sixth-order Butterworth type optical filter incurs in about 1.5 dB penalty with respect to an ideal one. All curves in Figs. 13 and 14 required about a minute of running time on a relatively fast processor and we point out that there is no other theory available in the literature from which they can be derived.

As regards of numerical results, we point out that our primary intention in this section is to demonstrate the potential of our method which may easily provide results for any practical situation.

VI. Conclusion

A novel approach for the analytical evaluation of the bit error probability of a preamplified direct detection system has been presented. It can take into account arbitrary pulse shapes and filtering and therefore permits to analyze the effects of chromatic dispersion, chirping and pre- and postdetection filter combinations. The saddle point integration method allows for a fast and reliable evaluation of the bit error probability. For example, all the performance curves shown were obtained with a program that automatically searches for the optimum threshold with three figures accuracy in a time variable from about 1–2 min on a SPARC processor. The computational burden is essentially a slowly increasing function of M in (A.5) and also depends on the fact that the integrals in (25) and (26) can be performed along the steepest descent path or should be done along a straight line through the saddle point. Much faster times can be achieved when using the saddle point approximation with practically no loss of accuracy. It has been shown that the eye closure penalty criterion is too optimistic in that it predicts substantially lower penalties than the real ones.

Appendix A

In this Appendix we give an expression for the sample $y(t_k)$ at the input of the decision device of Fig. 2.

By retaining only the nonnegligible harmonics, the quadratic detector input signal component is

$$s(t) = \sum_{\ell=-L}^{L} s_\ell e^{j2\pi\ell t/NT} \tag{A.1}$$

where

$$L = \eta N B_{0N} T \tag{A.2}$$

$$s_\ell = x_\ell H_f\left(\frac{\ell}{NT}\right) H_0\left(\frac{\ell}{NT}\right) \tag{A.3}$$

and x_ℓ are as in (8). The value of η to be used in (A.2) depends on the optical filter shape and may be chosen such that

$\sum_{|\ell|>L}|s_\ell|^2 < \varepsilon E_b$, with ε small enough, or may be found by successive trials. We found that a value of $\varepsilon \approx 10^{-4} \div 10^{-5}$ is more than safe in any practical situation.

As regards the quadratic detector input noise we can write it as

$$n(t) = \sum_{m=-M}^{M} n_m e^{j2\pi m(t-t_k+T_0)T_0} \quad \text{for } t_k - T_0 \le t \le t_k \tag{A.4}$$

where

$$M = \eta B_{0N} T_0 \tag{A.5}$$

$$n_m = w_m H_0\left(\frac{m}{T_0}\right) \tag{A.6}$$

and w_m are as in (9). Then the quadratic detector output signal, in the time interval $t_k - T_0 \le t \le t_k$, may be written as

$$\begin{aligned}|s(t)+n(t)|^2 = &\sum_{\ell=-2L}^{2L} c_\ell e^{j2\pi\ell t/NT} + \sum_{\ell=-L}^{L}\sum_{m=-M}^{M} s_\ell n_m^* \\ &\cdot \exp\left\{j2\pi\left[\frac{\ell t}{NT} - \frac{m(t-t_k+T_0)}{T_0}\right]\right\} \\ &+ \sum_{\ell=-L}^{L}\sum_{m=-M}^{M} s_\ell^* n_m \\ &\cdot \exp\left\{-j2\pi\left[\frac{\ell t}{NT} - \frac{m(t-t_k+T_0)}{T_0}\right]\right\} \\ &+ \sum_{\ell=-M}^{M}\sum_{m=-M}^{M} n_\ell n_m^* \\ &\cdot \exp\left\{j2\pi(\ell-m)\frac{t-t_k+T_0}{T_0}\right\}. \end{aligned} \tag{A.7}$$

c_ℓ being the autocorrelation of the coefficients of the Fourier series expansion of the signal $s(t)$ in (A.1)

$$c_\ell = \sum_{k=\max(-L,\ell-L)}^{\min(L,\ell+L)} s_k s_{k-\ell}^*. \tag{A.8}$$

After filtering by $H_R(f)$ and sampling, the sample $y(t_k)$ may be written as

$$\begin{aligned} y(t_k) = &\sum_{\ell=-2L}^{2L} c_\ell H_R\left(\frac{\ell}{NT}\right) e^{j2\pi\ell t_k/NT} \\ &+ \sum_{\ell=-L}^{L}\sum_{m=-M}^{M} s_\ell n_m^* H_R\left(\frac{\ell}{NT} - \frac{m}{T_0}\right) e^{j2\pi\ell t_k/NT} \\ &+ \sum_{\ell=-L}^{L}\sum_{m=-M}^{M} s_\ell^* n_m H_R^*\left(\frac{\ell}{NT} - \frac{m}{T_0}\right) e^{-j2\pi\ell t_k/NT} \\ &+ \sum_{\ell=-M}^{M}\sum_{m=-M}^{M} n_\ell n_m^* H_R\left(\frac{\ell-m}{T_0}\right) \end{aligned} \tag{A.9}$$

or, in compact matrix notation, as

$$y(t_k) = \mathbf{n}^{T*} Q \mathbf{n} + \mathbf{n}^{T*}\mathbf{v} + \mathbf{v}^{T*}\mathbf{n} + c \tag{A.10}$$

where $\mathbf{n}$ is a column vector whose $2M+1$ components are

$$n_i = w_{i-M-1} H_0\left(\frac{i-M-1}{T_0}\right) \qquad i = 1, 2, \cdots, 2M+1. \tag{A.11}$$

w_i being as in (9), Q is a $(2M+1)\times(2M+1)$ matrix whose elements are

$$q_{ij} = H_R\left(\frac{i-j}{T_0}\right) \qquad i, j = 1, 2, \cdots, 2M+1 \tag{A.12}$$

and, for the Hermitian symmetry of $H_R(f)$, they are such that $q_{ij} = q_{ji}^*$ (i.e. Q is Hermitian), $\mathbf{v}$ is a column vector whose $2M+1$ components are

$$v_i = \sum_{\ell=-L}^{L} s_\ell H_R\left(\frac{\ell}{NT} - \frac{i-M-1}{T_0}\right) e^{j2\pi\ell t_k/NT} \quad i = 1, 2, \cdots, 2M+1 \tag{A.13}$$

and finally c is the constant

$$c = \sum_{\ell=-2L}^{2L} c_\ell H_R\left(\frac{\ell}{NT}\right) e^{j2\pi\ell t_k/NT}. \tag{A.14}$$

Notice that $\mathbf{n}$ is a complex Gaussian random vector with zero mean and diagonal covariance matrix

$$E\{\mathbf{n}^*\mathbf{n}^T\} = 2\sigma^2 \mathrm{diag}\{|h_i|^2\} \tag{A.15}$$

where σ^2 is as in (10), $\mathrm{diag}\{c_i\}$ is by definition a diagonal matrix whose diagonal elements c_{ii} are $c_{ii} = c_i$, $i = 1, 2, \cdots$, and

$$h_i \triangleq H_0\left(\frac{i-M-1}{T_0}\right). \tag{A.16}$$

As the statistics of the filtered noise do not depend on the optical filter phase response but only on its amplitude response, by convenience we can define the matrix H as follows

$$H \triangleq \mathrm{diag}\{|h_i|\} \tag{A.17}$$

and by using the transformation

$$\mathbf{n} = H\mathbf{w} \tag{A.18}$$

(where the equal sign is to be interpreted in the sense that both sides are statistically equivalent) we may write

$$\mathbf{n}^{T*} Q \mathbf{n} = \mathbf{w}^{T*} H^{T*} Q H \mathbf{w} = \mathbf{w}^{T*} A \mathbf{w} \tag{A.19}$$

with

$$A = H^{T*} Q H \tag{A.20}$$

still Hermitian [27]. Since the matrix A accounts for the noise $\times$ noise contribution after the postdetection filter and at the output of the quadratic detector the noise $\times$ noise term is positive, then if the postdetection filter impulse response is always positive such is the noise $\times$ noise contribution and then A is positive definite [27], otherwise it may not. In either case, being A Hermitian, the eigenvalues of A are real (all positive if A is positive definite) and its eigenvectors orthogonal even if the eigenvalues are not all distinct [27]. If $H_0(f)$ is null at some discrete frequencies, then it may happen that A is singular, but this is not a problem as it is always possible to find a sequence of increasing values of μ in (28) for which this does not occur [if $H_0(f)$ is an ideal lowpass filter, then by the choice $\eta = 1$ this never happens]. So A can be diagonalized by the unitary matrix U formed

by its normalized eigenvectors arranged in the same order of their corresponding eigenvalues λ_i

$$A = U\Lambda U^{T*} \tag{A.21}$$

where

$$\Lambda = \mathrm{diag}\{\lambda_i\}. \tag{A.22}$$

Then we can write

$$\mathbf{n}^{T*}Q\mathbf{n} = \mathbf{w}^{T*}U\Lambda U^{T*}\mathbf{w} = \mathbf{z}^{T*}\Lambda\mathbf{z} \tag{A.23}$$

with

$$\mathbf{z} = U^{T*}\mathbf{w} = U^{T*}H^{-1}\mathbf{n} \tag{A.24}$$

and

$$E\{\mathbf{z}^*\mathbf{z}^T\} = 2\sigma^2 I \tag{A.25}$$

which means that the $\mathbf{z}$ components are independent complex Gaussian r.v. with zero mean and same variance. By defining the vector

$$\mathbf{b} \triangleq U^{T*}H^{T*}\mathbf{v} \tag{A.26}$$

and summing and subtracting to (A.10) the term $\mathbf{b}^{T*}\Lambda^{-1}\mathbf{b}$, the sample $y(t_k)$ may be written as

$$\begin{aligned} y(t_k) &= \mathbf{z}^{T*}\Lambda\mathbf{z} + \mathbf{z}^{T*}\mathbf{b} + \mathbf{b}^{T*}\mathbf{z} + c + \mathbf{b}^{T*}\Lambda^{-1}\mathbf{b} - \mathbf{b}^{T*}\Lambda^{-1}\mathbf{b} \\ &= (\mathbf{z} + \Lambda^{-1}\mathbf{b})^{T*}\Lambda(\mathbf{z} + \Lambda^{-1}\mathbf{b}) + c - \mathbf{b}^{T*}\Lambda^{-1}\mathbf{b} \\ &= \sum_{i=1}^{2M+1} \lambda_i \left| z_i + \frac{b_i}{\lambda_i} \right|^2 + \sum_{\ell=-2L}^{2L} c_\ell H_R \\ &\quad \cdot \left(\frac{\ell}{NT}\right) e^{j2\pi\ell t_k/NT} - \sum_{i=1}^{2M+1} \frac{|b_i|^2}{\lambda_i}. \end{aligned} \tag{A.27}$$

The above expression represents the final results of our calculations showing that $y(t_k)$ is composed by a signal term (the middle one) and two noise terms (the first and last ones).

As a quick check for our results, let us consider the fiber as nondispersive, i.e., $H_f(f) = 1$, $H_R(f)$ as a short-term integrator over the bit time T, $H_0(f)$ as an ideal filter of bandwidth $B_{0N} = M/T$ with $M \gg 1$ so that the duration of its impulse response is negligible with respect to T, and a one-shot transmission, i.e. $x(t)$ is a NRZ pulse which is described by (7) with $N = 1$ only in an interval equal to $T_0 = T$. Then Q, H, A, Λ and U become the identity matrix I, i.e., $\lambda_i = 1$ for all i and $\mathbf{b} = \mathbf{v}$, the constant c in (A.14) becomes $c = c_0$ and $\mathbf{b}^{T*}\Lambda^{-1}\mathbf{b} = \mathbf{v}^{T*}\mathbf{v} = c_0$, so the last two terms in (A.27) cancel each other and the sample becomes

$$y(t_k) = \sum_{i=1}^{2M+1} |z_i + x_i|^2 \tag{A.28}$$

which confirms the result of [5], valid only for this simplified case.

APPENDIX B

In this Appendix we detail the numerical evaluation of (25) and (26) by the saddle point method.

The probability density function $p_{n_k}(\tau)$ of n_k in (14) may be evaluated from its MGF $\Psi_{n_k}(s)$ in (16) as

$$\begin{aligned} p_{n_k}(\tau) &= \frac{1}{2\pi j}\int_{u_0-j\infty}^{u_0+j\infty} \Psi_{n_k}(s)e^{-s\tau}\,ds \\ &\quad -\frac{1}{\max|\beta_i^-|} < u_0 < \frac{1}{\max\beta_i^+}. \end{aligned} \tag{B.1}$$

Denoting by $u(x)$ the unit step function and using (B.1), we have for the left-hand tail probability

$$\begin{aligned} P\{n_k < \xi_k\} &= \int_{-\infty}^{\xi_k} p_{n_k}(\tau)\,d\tau \\ &= \int_{-\infty}^{\infty} p_{n_k}(\tau)u(\xi_k - \tau)\,d\tau \\ &= \frac{1}{2\pi j}\int_{u_0-j\infty}^{u_0+j\infty} \Psi_{n_k}(s) \\ &\quad \cdot \left(\int_{-\infty}^{\infty} u(\xi_k - \tau)e^{-s\tau}\,d\tau\right) ds \\ &= -\frac{1}{2\pi j}\int_{u_0-j\infty}^{u_0+j\infty} \frac{\Psi_{n_k}(s)}{s}e^{-s\xi_k}\,ds \\ &\quad -\frac{1}{\max|\beta_i^-|} < u_0 < 0 \end{aligned} \tag{B.2}$$

where the restriction on the u_0 range is necessary for the convergence of the inner integral in the second last equation in (B.2). In similar manner, the right-hand tail probability may be evaluated as

$$\begin{aligned} P\{n_k > \xi_k\} &= \int_{\xi_k}^{\infty} p_{n_k}(\tau)\,d\tau \\ &= \int_{-\infty}^{\infty} p_{n_k}(\tau)u(\tau - \xi_k)\,d\tau \\ &= \frac{1}{2\pi j}\int_{u_0-j\infty}^{u_0+j\infty} \Psi_{n_k}(s) \\ &\quad \cdot \left(\int_{-\infty}^{\infty} u(\tau - \xi_k)e^{-s\tau}\,d\tau\right) ds \\ &= \frac{1}{2\pi j}\int_{u_0-j\infty}^{u_0+j\infty} \frac{\Psi_{n_k}(s)}{s}e^{-s\xi_k}\,ds \\ &\quad 0 < u_0 < \frac{1}{\max\beta_i^+}. \end{aligned} \tag{B.3}$$

As the line integral of an analytic function does not depend on the integration path, we rewrite (B.2) and (B.3) as

$$P\{n_k < \xi_k\} = -\frac{1}{2\pi j}\int_{C_-} \frac{\Psi_{n_k}(s)}{s}e^{-s\xi_k}\,ds \tag{B.4}$$

$$P\{n_k > \xi_k\} = \frac{1}{2\pi j}\int_{C_+} \frac{\Psi_{n_k}(s)}{s}e^{-s\xi_k}\,ds \tag{B.5}$$

where the integration contours $C_\pm$ are conveniently chosen to closely approximate the paths of steepest descent passing through the saddle points $u_0^\pm$ of the integrands on the real s-axis. Rewriting the integrands of (B.4) and (B.5) as

$$\frac{\Psi_{n_k}(s)}{s}e^{-s\xi_k} = e^{\Phi_{n_k}(s)} \tag{B.6}$$

with

$$\Phi_{n_k}(s) = \log \Psi_{n_k}(s) - \log(s) - s\xi_k = \sum_{i=1}^{2M+1} \left[\frac{\alpha_i s}{1-\beta_i s} - \log(1-\beta_i s) \right] - \log(s) - s\xi_k \tag{B.7}$$

the saddle points u_0^- and u_0^+ are the roots of

$$\Phi'_{n_k}(s) = \sum_{i=1}^{2M+1} \frac{\alpha_i + \beta_i(1-\beta_i s)}{(1-\beta_i s)^2} - \frac{1}{s} - \xi_k = 0 \tag{B.8}$$

where $\Phi'_{n_k}(s)$ is the derivative of $\Phi_{n_k}(s)$. The saddle points are to be found numerically using, for example, the Newton's method. Starting with $s = s_0$ (real), the saddle points are the limit of the succession

$$s_{n+1} = s_n - \frac{\Phi'_{n_k}(s_n)}{\Phi''_{n_k}(s_n)} \tag{B.9}$$

where

$$\Phi''_{n_k}(s) = \sum_{i=1}^{2M+1} \frac{2\alpha_i\beta_i + \beta_i^2(1-\beta_i s)}{(1-\beta_i s)^3} + \frac{1}{s^2}. \tag{B.10}$$

As explained in [19], a convenient starting value s_0 is that derived by approximating n_k as a Gaussian r.v. with mean η_{n_k} (19) and variance $\sigma^2_{n_k}$ (20)

$$s_0 = \frac{\xi_k - \eta_{n_k} \pm \sqrt{(\xi_k - \eta_{n_k})^2 + 4\sigma^2_{n_k}}}{2\sigma^2_{n_k}} \tag{B.11}$$

where the $+$ sign is to be used for u_0^+ and the $-$ sign for u_0^-. If s_0 turns out to be outside the allowable range $-(1/\max|\beta_i^-|) < s_0 < 1/\max\beta_i^+$, one simply takes $s_0 = \pm(0.99/\max|\beta_i^\pm|)$. The iteration (B.9) can be stopped when $|s_{n+1} - s_n|$ falls below a prescribed value.

The paths of steepest descent $C_\pm$ are well approximated by parabolas of the form

$$s = u_0^\pm + \tfrac{1}{2}\kappa v^2 + jv, \qquad s = u + jv \tag{B.12}$$

where [19]

$$\kappa = \frac{\Phi'''_{n_k}(u_0^\pm)}{3\Phi''_{n_k}(u_0^\pm)} \tag{B.13}$$

$$\Phi'''_{n_k}(s) = \sum_{i=1}^{2M+1} \frac{6\alpha_i\beta_i^2 + 2\beta_i^3(1-\beta_i s)}{(1-\beta_i s)^4} - \frac{2}{s^3}. \tag{B.14}$$

The integrals (B.4) and (B.5) are then written as

$$P\{n_k \gtrless \xi_k\} = \pm\frac{1}{\pi}\int_0^\infty \Re\mathrm{e}\left\{ e^{\Phi_{n_k}(u_0^\pm + (1/2)\kappa v^2 + jv)}(1 - j\kappa v) \right\} dv \tag{B.15}$$

and are evaluated by the trapezoidal rule

$$P\{n_k \gtrless \xi_k\} \simeq \pm\frac{\Delta v}{\pi}\left[\frac{1}{2}f(0) + \sum_{n=1}^{\infty} f(n\Delta v) \right] \tag{B.16}$$

$$f(v) = \Re\mathrm{e}\left\{ e^{\Phi_{n_k}(u_0^\pm + (1/2)\kappa v^2 + jv)}(1 - j\kappa v) \right\}.$$

The sum is stopped when $f(n\Delta v)$ becomes negligible while the initial step size is taken as [19]

$$\Delta v = \frac{1}{\sqrt{2\Phi''_{n_k}(u_0^\pm)}} \tag{B.17}$$

and successively halved until the result stabilizes in the desired number of digits. By using the trapezoidal rule, when halving the step size, one can simply add to the previously accumulated trapezoidal sum the values of the integrand at the intermediate sampling points before multiplication by the final step size Δv. The advantage of this quadrature formula for infinite integrals of analytic functions is that the number of reliable significant figures approximately doubles when the step size is halved [28], [2929]. All the results in this work were evaluated with four reliable significant digits which needed the evaluation of a total of 30–50 samples for each symbol in the sequence $\{a_n\}$ even for probabilities down 10^{-16}.

When ξ_k in (22) is near η_{n_k} in (19) and when the saddle point is $u_0^+ > 0$, the path of steepest descent may be different from the parabola (B.12) in that it initially goes as (B.12) predicts with an initial curvature $\kappa < 0$, then the curvature changes sign and the path approaches another parabola with positive curvature but with its axis parallel instead that coincident with the real s-axis. In this case, integrating along the path (B.12) would cause the integral (B.15) to diverge. So, when κ in (B.13) turns out negative it should be set to zero in order to perform the integral in (B.15) along a straight vertical path. In a case such as this, it may be also numerically convenient to rewrite (B.7) as

$$\Phi_{n_k}(s) = \sum_{i=1}^{2M+1} \left[\frac{\alpha_i\beta_i s^2}{1-\beta_i s} - \log(1-\beta_i s) - \beta_i s \right] - \log(s) + (\eta_{n_k} - \xi_k)s. \tag{B.18}$$

When the postdetection filter has an impulse response which changes sign, i.e., when the matrix A in (A.20) is not definite positive, then the saddle point may be too near the closest singularity on its right for the trapezoidal sum to have the chance of converging before the parabola approximating the steepest descent path crosses the boundaries of the regularity domain. This can be detected by the fact that the integrand diverges and when this happens the integration must be stopped and performed again along a straight vertical path through the saddle point by setting κ in (B.13) to zero.

ACKNOWLEDGMENT

The author wishes to thank A. Bononi, G. Picchi, R. Raheli (University of Parma) and particularly G. Prati (Scuola Superiore S. Anna—Pisa) for their helpful suggestions and comments during the preparation of this paper and one anonymous reviewer for suggesting several improvements to the paper and bringing to his attention the work by Helstrom in [12].

REFERENCES

[1] P. S. Henry, "Error-rate performance of optical amplifiers," in *Tech. Dig. OFC'89*, Houston, TX, Feb. 1989, Paper THK3.

[2] D. Marcuse, "Derivation of analytical expressions for the bit-error probability in lightwave systems with optical amplifiers," *J. Lightwave Technol.*, vol. 8, no. 12, pp. 1816–1823, Dec. 1990.

[3] O. K. Tonguz and L. G. Kazovsky, "Theory of direct-detection lightwave receivers using optical amplifiers," *J. Lightwave Technol.*, vol. 9, pp. 174–181, Feb. 1991.
[4] D. Marcuse, "Calculation of bit-error probability for a lightwave system with optical amplifiers and post-detection Gaussian noise," *J. Lightwave Technol.*, vol. 9, pp. 505–513, Apr. 1991.
[5] P. A. Humblet and M. Azizoğlu, "On the bit error rate of lightwave systems with optical amplifiers," *J. Lightwave Technol.*, vol. 9, pp. 1576–1582, Nov. 1991.
[6] J.-S. Lee and C.-S. Shim, "Bit-error-rate analysis of optically preamplified receivers using an eigenfunction expansion method in optical frequency domain," *J. Lightwave Technol.*, vol. 12, pp. 1224–1229, July 1994.
[7] N. G. Jensen, E. Bodtker, G. Jacobsen, and J. Strandberg, "Performance of preamplified direct detection systems under influence of receiver noise," *IEEE Photon. Technol. Lett.*, vol. 6, pp. 1488–1490, Dec. 1994.
[8] L. F. B. Ribeiro, J. R. F. Da Rocha, and J. L. Pinto, "Performance evaluation of EDFA preamplified receivers taking into account intersymbol interference," *J. Lightwave Technol.*, vol. 13, pp. 225–232, Feb. 1995.
[9] S. L. Danielsen, B. Mikkelesen, T. Durhuus, C. Joergensen, and K. E. Stubkjaer, "Detailed noise statistics for an optically preamplified direct detection receiver," *J. Lightwave Technol.*, vol. 13, pp. 977–981, May 1995.
[10] C. Lawetz and J. C. Cartledge, "Performance of optically preamplified receivers with Fabry–Perot optical filters," *J. Lightwave Technol.*, vol. 14, pp. 2467–2474, Nov. 1996.
[11] I. T. Monroy and G. Einarsson, "Bit error evaluation of optically preamplified direct detection receivers with Fabry–Perot optical filters," *J. Lightwave Technol.*, vol. 15, pp. 1546–1553, Aug. 1997.
[12] C. W. Helstrom, "Distribution of the filtered output of a quadratic rectifier computed by numerical contour integration," *IEEE Trans. Inform. Theory*, vol. IT-32, pp. 450–463, July 1986.
[13] H. Meyr, M. Moeneclaey, and S. A. Fechtel, *Digital Communication Receivers*. New York: Wiley, 1998.
[14] G. P. Agrawal, *Nonlinear Fiber Optics*. San Diego, CA: Academic, 1989.
[15] S. W. Golomb, *Shift Register Sequences*. San Francisco, CA: Holden-Day, 1967.
[16] H. Van Trees, *Detection, Estimation, and Modulation Theory, Part I*. New York: Wiley, 1968.
[17] J. G. Proakis, *Digital Communications*. New York: McGraw-Hill, 1983.
[18] C. W. Helstrom and J. A. Ritcey, "Evaluating radar detection probabilities by steepest descent integration," *IEEE Trans. Aerospace Electron. Syst.*, vol. 20, pp. 624–634, Sept. 1984.
[19] C. W. Helstrom, *Statistical Theory of Signal Detection*. Elmsford, NY: Pergamon, 1968.
[20] S. Benedetto, E. Biglieri, and V. Castellani, *Digital Transmission Theory*. London, U.K.: Prentice-Hall, 1987.
[21] A. F. Elrefaie, R. E. Wagner, D. A. Atlas, and D. G. Daut, "Chromatic dispersion limitations in coherent lightwave transmission systems," *J. Lightwave Technol.*, vol. 6, pp. 704–709, May 1988.
[22] L. J. Cimini, L. J. Greenstein, and A. A. M. Saleh, "Optical equalization to combat the effects of laser chirp and fiber dispersion," *J. Lightwave Technol.*, vol. 8, pp. 649–659, May 1990.
[23] F. Bruyère, "Impact of first- and second-order PMD in optical digital transmission systems," *Optical Fiber Technol.*, no. 2, pp. 269–280, 1996.
[24] K. Yonenaga and S. Kuwano, "Dispersion-tolerant optical transmission system using duobinary transmitter and binary receiver," *J. Lightwave Technol.*, vol. 15, pp. 1530–1537, Aug. 1997.
[25] K. Hinton, "Dispersion compensation using apodized Bragg fiber gratings in transmission," *J. Lightwave Technol.*, vol. 16, pp. 2336–2346, Dec. 1998.
[26] S. D. Personick, "Receiver design for digital fiber optic communication systems, I," *Bell Syst. Tech. J.*, vol. 52, no. 6, pp. 843–874, July 1973.
[27] S. Perlins, *Theory of Matrices*. New York: Dover, 1991.
[28] C. Schwartz, "Numerical integration of analytic functions," *J. Computat. Phys.*, vol. 4, pp. 19–29, 1969.
[29] S. O. Rice, "Efficient evaluation of integrals of analytic functions by the trapezoidal rule," *Bell Syst. Tech. J.*, vol. 52, pp. 707–722, May–June 1973.

Enrico Forestieri (M'92) was born in Milazzo, Italy, in 1960. He received the Dr.Ing. degree in electrical engineering from the University of Pisa, Pisa, Italy, in 1988.

From 1989 to 1991 he was a Postdoctoral Scholar at the University of Parma, Italy, working in optical communication systems. Since November 1991 he has been a Research Scientist and Faculty Member of the University of Parma. His research interests include digital communication theory and optical communication systems.